INTERNAL STRUCTURE MODELLING OF EUROPA.

C. Thomas. Institute of Ocean Sciences, 9860 West Saanich Road, Sidney, British Columbia, Canada V8L 4B2 (ThomasC@pac.dfo-mpo.gc.ca)

The gravity data gathered by the Galileo Orbiter from close satellite flybys of Europa provide several important constraints to the possible internal structures of this satellite. Anderson *et al.* [1] derived three-layer models by calculating analytical solutions to Clairaut's equation. Here, I present four-layer (ice, saltwater, silicate mantle, Fe-FeS core) models of Europa determined by empirical modelling of the satellite's interior.

The SATMOD moment of inertia program

The SATMOD (SATellite MODeller) FORTRAN program was designed to construct accurate models of the interior structure of satellites, and to more fully explore the range of possible models for those bodies. It can potentially be used to construct similar models for any spherical planetary body for which the relevant basic physical parameters are known.

The observed values of radius, mass, density, and moment of inertia factor (C/MR^2) for the body in question (and 1σ error bars for these values) are first entered into SATMOD – in the case of Europa, these are taken from [1]. Appropriate layer materials are then entered (e.g. ice I, saltwater, silicate, Fe-FeS), along with the uncompressed density, bulk modulus and percentage of satellite mass that each material represents.

SATMOD constructs a range of possible models by calculating the radius, mass, bulk density and C/MR^2 of the satellite given the properties of the layers entered into the program. It also accounts for self-compression of layers due to the mass of overlying material (i.e. increasing density with depth) and the variation in gravitational acceleration with depth in the body. The resulting physical parameters of the model are then compared with the values derived from Galileo Orbiter observations [1]. Where appropriate, the density of individual layers (i.e. more hydrated/lower density silicates, more salty/higher density saltwater oceans) can also be varied over a user-defined range of values which means that the models are recalculated for all layer densities as well as for every permutation of layer mass. If the calculated values of the predicted parameters fall within the error bounds of the observed values, the resulting model and associated data are output to a text file; if the calculated values fall beyond the error bounds of the observed values, the model is discarded.

Other constraints are also applied in order to discard unrealistic models: four layers must exist in the output model (i.e. the mass of each layer must be greater than 0%); the core cannot contain greater than 50% of the mass of the body since such a massive FeS core would be geochemically unreasonable; a layer with a higher density cannot overlie one with a lower density; and the pressures at the base of layers must be appropriate to allow for the existence of the material present there (e.g. the various high pressure ice phases).

SATMOD produces physical models that are constrained solely by moment of inertia, radius, density and mass. No chemical modelling is carried out as part of the model verification - though this can be carried out on the results afterwards. However, care is taken to assume reasonable densities for materials comprising the layers and to use appropriate physical parameters. It should also be noted that SATMOD does not account for any variation in the bulk modulus of the material with pressure and temperature.

In addition, some thermal modelling is also performed to further limit the range of models. While a model may appear to be physically valid, it is not necessarily *realistic* - the heat flow determined from a model may be unreasonably high or low to produce the model structure. Radiogenic heating can be determined from the thickness of the Ice I shell and the percentage mass of silicate in the model (we assume that all the radiogenic heat is produced in the silicate mantle). From this we can calculate a 'silicate heat density' - the heat produced by each kilogram of silicate material to result in that ice thickness. This silicate heat density is compared to chondritic values from [2] (assumed to be 4.5 x 10^{-12} W kg^{-1}). The radiogenic heat production of Europa is uncertain (since it is dependent on composition), we arbitrarily assume that models with greater than 500% or less than 10% of the chondritic silicate heat density are too extreme - these models are rejected. At present, SATMOD only attempts to account for radiogenic heating - tidal heating is ignored for now.

More often than not many thousands or even millions of valid models are produced, depending on the range of parameters and the size of the variable increments used. By taking a wide range of factors and increments and (where appropriate) layer densities, it is possible to identify peaks in the distribution of valid models and to select promising models from them that fit the observed parameters. It is difficult to pick out one single model to highlight - all the output models agree with observed parameters/constraints and are therefore all potentially valid. In practice, there is a peak in distribution of the number of models at a specific combination of water and silicate density, so we focus on models with those parameters. Note that this peak is not the most *likely* set of models that is produced - it is simply the most numerous. Any models selected for closer examination are therefore non-unique.

Results

Table 1 shows the parameters entered into SATMOD to generate the four-layer models of Europa with an Fe-FeS core produced here.

Table 1: Input parameters: Fe-FeS core

Target Mass	4.79982 x 10^{22} kg
Target Radius	1560.7 ± 0.65 km
Target Density	3014.44 ± 3.4 kg m^{-3}
Target C/MR² factor	0.347447 ± 0.0062

LAYERS	**ρ_u (kg m^{-3})**	**K (GPa)**	**%mass variability**
Ice I	921	9.2	0.1 - 15.1 (0.1)
Salt Water	1010 - 1300 (10)	3.0	0.2 - 30.2 (0.1)
Silicate Mantle	3000 - 4000 (10)	235.0	53.2 - 98.8 (7.6)
Fe-FeS Core	5150	120.0	(remainder)

Target values taken from [1]. **ρ_u** = uncompressed density, **K** = (uncompressed) bulk modulus. Numbers in parentheses are the increments by which the density and mass% values vary in the models. Silicate and FeS Bulk Modulus values are taken from [3]. The saltwater and silicate densities reflect varying compositions of those materials - higher saltwater densities represent higher salinity water, whereas higher density silicate represent less hydrated silicates.

The numerical distribution of four-layer models produced by SATMOD is shown in Figure 1. In this figure, the uncompressed density of the saltwater layer (denser water is more saline) is plotted against the uncompressed density of the silicate layer (denser silicates are less hydrated). The grey scale represents the number of valid models produced that have that combination of densities. All the models have the same Ice I and Fe-FeS densities, although these are modified by self-compression.

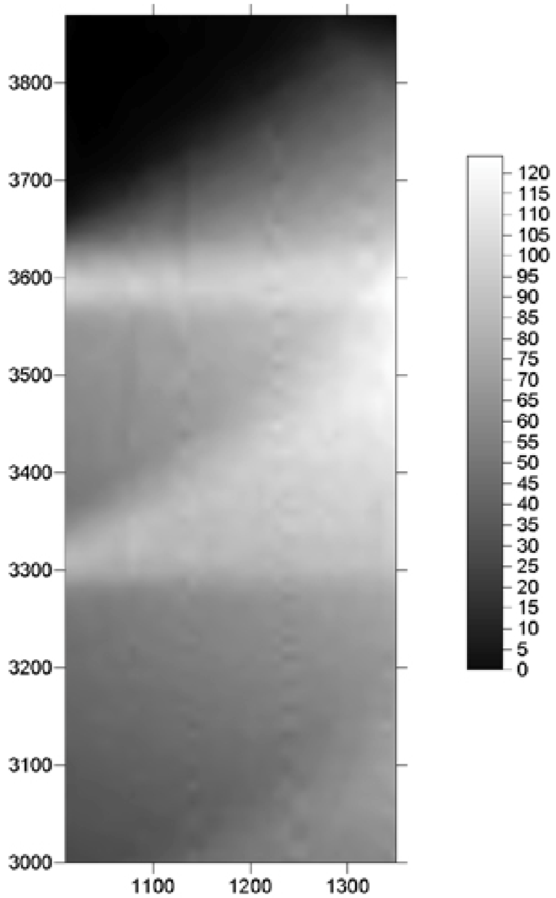

Figure 1: numerical distribution of models, shown as a rock density (left) vs. ice density plot (bottom). Both axes are in units of kg m^{-3}. Greyscale bar indicates the number of models produced.

The fine- and medium-scale structure of the plotted surface is an artifact of the increment size of the step-like nature of the modelling process and the discreteness of the layer densities and mass percentages in the input. However, the general trend of the plots is always the same regardless of the input parameters - a gradual slope rising from low silicate densities towards a ‘ridge’ at 3600 kg m^{-3}, and a much steeper downward slope away towards low water and high silicate densities. Since this is common to all modelling runs regardless of the increment size, this is interpreted as a real characteristic of the solutions and cannot be noise. The largest number of models produced is at a silicate density of 3600 kg m^{-3} and a water density of 1350 kg m^{-3}, indicating a highly saline water layer and a dehydrated silicate layer (similar in density to Io). The liquid density is typical of a $MgSO_4$-H_2O mix with around 20-30% solute [4].

The three-layer models produced by [1] for an Fe-FeS core treat the ice and water layers as a single layer that ranges between 80 and 200 km in thickness. The average density of this layer is between 900 and 1300 kg m^{-3}, and the silicate density ranges between 3000 and 3800 kg m^{-3} (Anderson *et al.* rule out silicate densities below 3000 kg m^{-3} on physical and chemical grounds). The radius of the Fe-FeS core ranges from 0 to 50% of Europa’s radius, and the thickness of the ice+water layer ranges between 80 and 200 km.

Presented in similar terms to [1], our results indicate that the average compressed density of the combined ice+water layer is between 930 kg m^{-3} and 1379 kg m^{-3}, the compressed silicate density ranges between 3012 kg m^{-3} and 3926 kg m^{-3}, and the radius of the Fe-FeS core ranges from 18.3 to 52.4% of Europa’s radius (286 to 818 km). The combined thickness of the ice+water layers ranges between approximately 70 km for the models with lower silicate densities, up to 150 - 200 km thick for the higher silicate densities. As an aside, we also produced models for extremely low silicate densities (2500 - 3000 kg m^{-3}), and discovered that these had combined ice+water thicknesses of the order of 25 ± 5 km. Our models are therefore broadly in agreement with [1].

Splitting apart the ice and water layers in our models, the ice layer ranges between 17 km and 148 km thick and the water layer can be as thick as 192 km and as thin as 2.5 km. The thickest ice layers are associated with the thinnest water layer and vice versa - although there are plenty of intermediate models where the ice and water layers are much more similar in thickness. Some of the extreme models may not be physically realistic, however - most importantly, the ‘silicate heat density’ required to produce these thicknesses are themselves at the extreme ends of their range. The thick water layers buried beneath a thin ice layer have base pressures that are above those required for the Ice III transition, but the temperature at these depths is likely to be higher than the temperature at the based of the ice layer (~ 270 K), which would prevent this transition and keep the ocean liquid. At the other extreme, the water layer in the thick ice/thin water combination may be too thin to generate a magnetic field [5] - magnetic field measurements provide another constraint that can be incorporated into the model in later development. Furthermore, the surface geology may preclude models that are over a hundred kilometres thick.

It should also be noted that - for the 1350-3600 density combination at least - the thinnest (~ 17 km) ice models require radiogenic heat production rates that are nearly five times higher than that of the Earth today. Models with more earth-like levels of ‘silicate heat density’ have ice shells and water layers that are both approximately 80 km thick.

Further Work

These results are very much a work in progress - the models can be refined much further using higher resolution input parameters that require more computing time. More constraints remain to be added including those provided by induced magnetic field measurements, geology and tidal heating - all of these can further narrow down the field of valid, realistic models for Europa’s interior. The tidal heating would not be model-dependent and is constrained by scaling down the heating experienced by Io. According to [6] the tidal heating for Europa scales down to approximately 10% of that of Io, or approximately 10^{13} W - qualitatively, this extra heat source may significantly thin the ice shell to much less than 10 km in thickness. In addition, a more efficient system based on advanced multi-objective genetic algorithms [7] is currently being developed that shows promise, that we hope to present at a later date.

References

[1] Anderson *et al.* (1998), *Science*, **281**, 2019-2022.
[2] Spohn & Schubert (2003), *Icarus*, **161**, 456-467.
[3] *Basaltic Volcanism on the Terrestrial Planets* (1981). Pergamon Press, Inc., New York.
[4] Hogenboom *et al*. (1995), *Icarus*, **115**, 258-277.
[5] Zimmer *et al.* (2000), *Icarus*, **147**, 329-347.
[6] Thomson & Delaney (2001), *JGR Planets*, **106** (E6), 12335-12365.
[7] D. E. Goldberg (1989). *Genetic Algorithms in Search, Optimization, and Machine Learning*. Addison-Wesley Publishing Company.